Microwave generation of X-waves by means of a planar leaky-wave antenna

Microwave Generation of X-Waves by means of a Planar Leaky-Wave Antenna

D. Comite,[1] W. Fuscaldo,[1] S. K. Podilchak,[2] V. Gómez-Guillamón Buendía,[2] P. D. Hilario Re,[2] P. Baccarelli,[3] P. Burghignoli,[1] and A. Galli[1]

[1)] *Dipartimento di Ingegneria dell'Informazione, Elettronica e Telecomunicazioni, Università degli Studi di Roma Sapienza, via Eudossiana 18, 00184 Roma, Italy.*[a)]

[2)] *Institute of Sensors, Signals, and Systems, School of Engineering and Physical Sciences Edinburgh Campus, Heriot-Watt University, Edinburgh EH14 4AS, United Kingdom*

[3)] *Dipartimento di Ingegneria, Università Roma Tre, via Vito Volterra, 62, 00146, Roma, Italy.*

(Dated: 21 September 2018)

We analyze and experimentally demonstrate the possibility of generating X-waves at microwave and millimeter-wave frequencies by means of a partially open radial parallel-plate waveguide antenna. The structure is azimuthally symmetric and fed in the center by means of a simple vertical coaxial probe, which excites a cylindrical leaky wave. Radially periodic annular slots etched in the upper metal plate allow the propagation of a *backward* leaky wave, as required for generating Bessel beams in the near-field region. Since X-waves are polychromatic superpositions of Bessel beams, the wavenumber frequency dispersion of the relevant leaky mode is accounted for by the antenna design. In particular, a dispersion-engineering approach is used to properly select the operating fractional bandwidth for the antenna. Even if the beneficial effect of a large bandwidth is partially neutralized by the dispersive character of the resulting pulse, this being more prominent as the bandwidth increases, the experimental results demonstrate the capability of this simple planar design of generating X-waves in the microwave regime. The antenna can be of interest for the design of next-generation medical imaging devices, for non-destructive evaluations, as well as for wideband near-field secure communications and wireless power transfer systems at microwaves and millimeter waves.

PACS numbers: 63.20.Pw, 84.40.Ba, 41.20.Jb, 41.20.-q, 84.40.-x

There has been increasing interest, in the last decade, in the analysis and design of low-cost and low-profile microwave and millimeter-wave devices enabling the radiation of localized energy, in the form of nondiffracting waves[1–8]. Nondiffracting waves represent a wide class of solutions to the Helmholtz equation with remarkable limited-diffractive and limited-dispersive features[7–11], which make them a very attractive solution in the field of the wireless power transfer, imaging, as well as secure chip-to-chip and short-distance communications (see, e.g.,[7,8,12–17] and refs. therein).

Among the various types of nondiffracting waves, Bessel beams and X-waves represent the most known monochromatic solutions (i.e., beams) and polychromatic solutions (i.e., pulses), respectively[10,18–21]. The former can be represented as a superposition of plane waves whose direction lies on the surface of a cone[7]; the semi-aperture angle of such a cone is usually called the *axicon angle* (see Fig. 1). Interestingly, Bessel beams exhibit transverse energy localization up to a distance (the nondiffracting range, z_{NDR}) from the radiating aperture which is governed by the aperture radius ρ_{ap} and the axicon angle θ through the relation $z_{\mathrm{NDR}} = \rho_{\mathrm{ap}} \cot \theta$[22]. Experimental generations of Bessel beams have been reported so far in both the optical range (see, e.g.,[23] and refs. therein) and the microwave range (see, e.g.,[24]).

[a)] Electronic mail: {davide.comite,walter.fuscaldo}@uniroma1.it

On the other hand, X-waves are obtained as a weighted frequency superposition of Bessel beams sharing the same axicon angle[7,8]. Indeed, when the weight is uniform over the frequency spectrum, they can be interpreted as the time-domain inverse Fourier-transform of Bessel beams. As a result, they inherit the transverse localization of Bessel beams. In addition, X-waves also exhibit longitudinal energy localization up to the nondiffracting range. The level of longitudinal localization can be independently controlled by the fractional bandwidth over which X-waves are generated, provided that the structure exhibits limited *cone dispersion* (i.e., the variation of the axicon angle with frequency)[11].

Differently from Bessel beams[25], experimental evidences of X-waves are rather scarce. After their first realization in acoustics[26] in the early '90s, the first demonstrations in optics appeared at the end of the '90s[27,28]. Very recently, the experimental generation of X-waves in the microwave range has been demonstrated and discussed in[29]. Indeed, the device proposed in[29] resorts to a dielectric lens to avoid the *wavenumber dispersion* (and, consequently, cone dispersion) typical of radial waveguides. This is paid at the expense of a bulky non-planar design. This temporary lack of evidence of X-waves in the microwave range is due to the inherent difficulties in designing broadband Bessel-beam launchers with limited dispersive features, as required to grant the localized character of X-waves[11,30].

On the other hand, the effects of *anomalous dispersion*

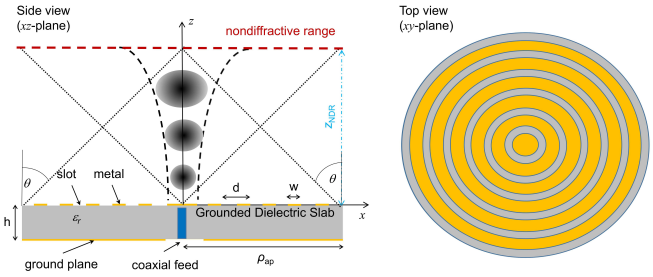

FIG. 1. Radially periodic leaky-wave antenna for the generation of X-waves at microwaves. The antenna is made by an annular, periodic, MSG placed on a dielectric laminate having low permittivity ($\epsilon_r = 2.2$). The antenna generates a bullet-like (i.e., focused) pulse within a confined region in front of the antenna. The X-wave section slowly increases beyond the nondiffracting range due to the controlled wavenumber dispersion. Antenna parameters: strip width $w = 4$ mm, period $d = 10$ mm, slab thickness $h = 3.14$ mm, radial aperture $\rho_{\rm ap} = 140$ mm.

in dielectric media in connection with the generation of X-waves have been extensively analyzed in optics[27,31–34]. We note that, while anomalous dispersion of dielectric media plays a key role for the generation of X-waves, *wavenumber* dispersion is an undesirable effect for their synthesis through radial waveguides[11,30,35]. In this regard, dispersion engineering approaches as those discussed in the following, can be beneficial to limit as much as possible the temporal broadening of the propagating pulse.[9]

Recently, different broadband planar radiators with limited dispersive features have been proposed in the microwave range[30,35–40]. The underlying idea, common to all wideband Bessel-beam launchers based on radial waveguides, is to synthesize an inward traveling-wave cylindrical distribution over the aperture plane, i.e.,

$$A_t(\rho, \phi, z = 0) = H_n^{(1)}(k_\rho \rho) e^{-jn\phi}, \quad \rho \leq \rho_{\rm ap}, \qquad (1)$$

where $\{\rho,\ \phi,\ z\}$ are the coordinates of a cylindrical reference frame, $k_\rho = \beta_\rho - j\alpha_\rho$ is the radial complex wavenumber, related to the vertical one (i.e., k_z) through the separation relation $k_\rho^2 + k_z^2 = k_0^2$, k_0 being the free-space wavenumber. $H_n^{(1)}(\cdot)$ represents the Hankel function of the first kind and n-th order, and A_t an aperture field (either electric or magnetic) of arbitrary polarization. A time dependence of the kind $e^{j\omega t}$ has been assumed and suppressed. It is well known[38,41,42] that such an aperture field allows for generating Bessel beams over a diamond-shaped region in front of the aperture and within the nondiffractive range.

Although it is possible to synthesize an inward aperture field of arbitrary azimuthal order through the holographic principle[24,36,43,44], we use here the leaky-wave theory to synthesize a zero-th order transverse magnetic (TM) Bessel beam for the vertical z-component of the electric field through a radially periodic leaky-wave antenna (LWA)[30,40]. In this case, an annular metal strip grating (MSG) is placed on top of a simple grounded dielectric slab (GDS) and fed in the center by a coaxial cable, which excites the fundamental TM cylindrical leaky mode (see Fig. 1). Therefore, the structure supports an aperture field exhibiting the desired inward character:

$$E_\rho(\rho, z = 0) = -j \frac{k_z}{k_\rho} E_0 H_0^{(1)'}(k_\rho \rho), \qquad (2)$$

where the prime symbol $(\cdot)'$ stands for the first derivative with respect to the argument. On this basis, the MSG has to be designed to excite a backward fast leaky wave[45] (i.e., with $-k_0 < \beta_\rho < 0$), so that the required inward character is recovered exploiting the well-known relation between Hankel functions, i.e., $H_0^{(2)}(k_\rho \rho) = -H_0^{(1)}(-k_\rho \rho)$[46]. As a result, the radiated electric field components take the following expression:

$$E_\rho(\rho, z) \propto J_0'(k_\rho \rho) u(\rho \cot\theta - z) u[(\rho_{\rm ap} - \rho)\cot\theta - z], \qquad (3)$$

$$E_z(\rho, z) \propto J_0(k_\rho \rho) u(\rho \cot\theta - z) u[(\rho_{\rm ap} - \rho)\cot\theta - z], \qquad (4)$$

for $\rho \leq \rho_{\rm ap}$ and $0 \leq z \leq z_{\rm ndr}$. $J_0(\cdot)$ represents the Bessel function of first kind and zero-th order and the prime symbol $(\cdot)'$ stands again for the first derivative with respect to the argument. The Heaviside step function $u(\cdot)$ accounts for the ray-optics description of the field within the nondiffractive range[42] (note also that $E_\phi = 0$, due to the azimuthal symmetry of the electric field). An extensive theoretical discussion on these aspects can be found in[30,36,42], whereas an experimental validation of the concept is given in[40]. Interestingly, the planar antenna in[40] exhibits a 40% impedance bandwidth, spanning from 14 GHz to 21 GHz, opening to the possibility of generating X-waves by means of such a low-cost and low-profile structure. The experimental demonstration of the time-domain focusing capabilities in terms of X-waves of the LWA proposed in[40] is investigated here.

In spite of the remarkably large impedance bandwidth of the considered antenna, the portion of the frequency range that can be used for the generation of X-waves is limited by the wavenumber dispersion, which is an inherent feature of LWAs. More importantly, we remind that only fast (i.e., radiating) backward waves may contribute to the generation of X-waves, hence the bandwidth is limited by the range in which $-k_0 < \beta_\rho < 0$. This corresponds to the *visible* range through the well-known relation $\beta_\rho = k_0 \sin\theta$. We should mention that periodic LWAs commonly experience degradation of the radiation in proximity of the open stopband (i.e., when $\beta_\rho \simeq 0$)[47]. Moreover, it is noted that for $\theta > 45°$, the nondiffractive range is less than the aperture radius. On this basis, depending on the considered structure, the operational frequency range should be practically narrowed between about $-0.8k_0 < \beta_\rho < -0.1k_0$, which corresponds for the structure under consideration here to a frequency interval ranging from 15 to 21.5 GHz[40]. Therefore, the intersection between the radiating and the impedance bandwidth

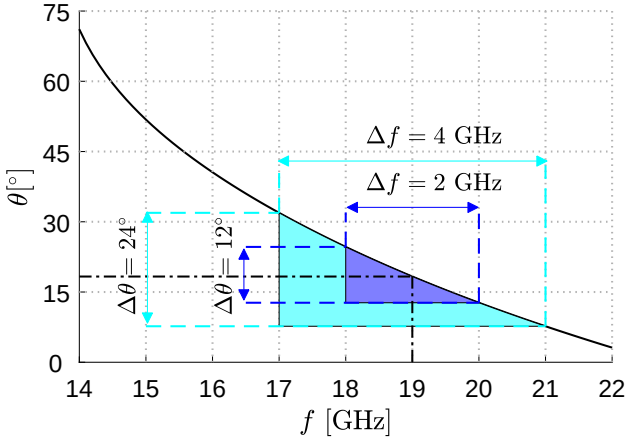

FIG. 2. Dispersion behavior of the axicon angle for the structure presented in Fig. 1. Two frequency bands are highlighted around the center frequency $f = 19$ GHz: the 18 to 20 GHz band (blue violet) and the 17 to 21 GHz band (light blue).

defines the available frequency range, which is given here by 15 to 21 GHz. The corresponding operative fractional bandwidth (FBW, about 30%) is still considerably large, and can be successfully exploited to generate X-waves. As a matter of fact, as recently discussed in[11], by increasing the FBW the longitudinal localization of the pulse is expected to improve. However, this feature holds rigorously true for nondispersive X-waves. Conversely, for dispersive X-waves[11], as those discussed here, wavenumber dispersion has a more detrimental effect as the FBW increases. Indeed, the leaky-wave dispersion could dramatically affect the longitudinal localization of the field, which, in the limit, can be neutralized by the dispersive character of the resulting pulse[11,30].

In this frame, larger operational FBWs do not necessarily correspond to an enhanced longitudinal localization of the pulse, as we will theoretically and experimentally discuss next. As shown in the dispersion plot of Fig. 2, if one takes a small symmetric frequency band around the center frequency $f_0 = 19$ GHz, the amount of cone dispersion $\Delta\theta$ is controlled by the dispersion curve. For example, in the frequency range 18 to 20 GHz, the structure experiences a cone dispersion of about $\Delta\theta = 12°$ over a FBW slightly greater than 10%, whereas in the frequency range 17 to 21 GHz, the structure experiences a cone dispersion of about $\Delta\theta = 24°$ over a FBW slightly greater than 20%. Clearly, as the FBW doubles, $\Delta\theta$ doubles as well, due to the almost linear dispersion behavior of the axicon angle. As a result, the expected increase in localization could be hindered by dispersion. This aspect has been analytically discussed in[30], and will be experimentally corroborated here by taking advantage of the measurement setup developed in[40]. We stress here that a similar frequency-domain technique has been recently validated for the first experimental generation of X-waves in the microwave range[29].

As given in[29,35], the i-component (with $i = \rho, z$) of the X-wave produced by the launcher is obtained by numerically performing the following integral

$$e_i(\rho,\phi,z;t) = \Re\left[\int_{\Delta\Omega} E_i^{\mathrm{mea}}(\rho,\phi,z;\omega)e^{j\omega t}d\omega\right], \qquad (5)$$

where E_i^{mea} is the electric field measured on a 2-D lattice (spatial steps of 3 mm) on the xz longitudinal plane in the near-field of the antenna and $\Delta\Omega = 2\pi\Delta f$ the considered bandwidth (see Fig. 2). From Eqs. (3)-(4) it can then be deduced that each component $e_i(\rho,\phi,z;t)$ is a spectral superposition of Bessel beams.

It is worth to stress here that a coherent processing has to be developed (i.e., retaining both amplitude and phase of the near-field distribution) to generate the X-wave; thus, the initial phase of the spectral field should be controlled by the experimental setup. For measurement simplicity, the maximum distance along the z-axis at which samples are collected is set here to be 35 cm, which approximately corresponds to the nondiffracting range, z_{NDR}, evaluated at the central frequency $f = 19$ GHz. Due to practical constraints, measurements have been collected starting from a minimum distance from the antenna aperture equal to 6 cm. To avoid sampling artifacts, such as unwanted replica and aliasing, a spectral sampling of 0.5 GHz is considered for the two frequency ranges, namely 17 to 21 GHz (9 frequency samples) and 18 to 20 GHz (5 frequency samples). In fact, considering a pulse propagating in free space, the time needed to travel the nondiffractive distance (corresponding to 35 cm here) is equal to $T_0 = z_{\mathrm{NDR}}/v_z$, where $v_z = \partial\omega/\partial\beta_z$ represents the group velocity of the pulse along the longitudinal direction. (Note that $v_z \simeq 0.64c$, c being the speed of light in vacuum). Hence, the number of frequency samples N_s has to be greater than $N_s = \lceil \Delta f T_0 + 1/2 \rceil$.

Experimental 2-D maps time-evolution for the ρ and z components of the electric field on the xz-plane have been reported in Figs. 3(a)-(f), considering the 17 to 21 GHz range. Figures 3(a)-(c) present the normalized time-domain distribution of e_ρ, whereas Figs. 3(d)-(f) are those of e_z. The localized nature of both the components of the pulse, which basically maintains its nondiffracting profile along both the transverse and longitudinal directions, can be observed. More importantly, the field clearly shows a limited-diffractive nature, despite the inherent dispersion of the leaky mode responsible for the X-wave radiation, which, as discussed, is connected to the dispersion of the axicon angle in Fig. 2. Note that the transverse profile of the pulse is dictated by the relevant Bessel function, as corroborated by the frequency-domain fields given by (3)-(4).

To assess the effect of the wavenumber dispersion on the profile of the nondiffracting pulse, Figs. 4(a)-(b) and Figs. 4(c)-(d) report the amplitude of e_ρ and e_z, respectively, at a fixed time instant but for two different values of FBW (see the caption for the relevant details). It can be observed that the bandwidth has an important effect on the shape of the pulse. Its spatial pro-

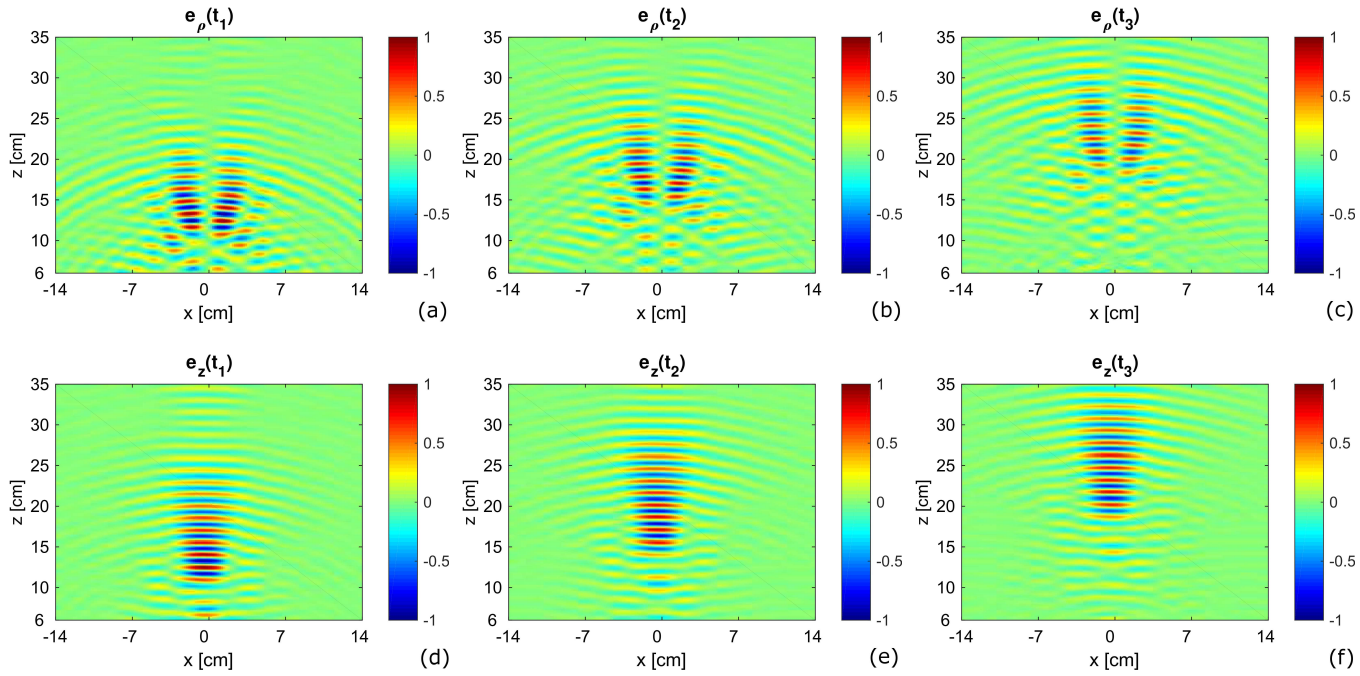

FIG. 3. Measured time evolution of the normalized field distributions of the structure of Fig. 1 for (a)-(c) the ρ-component and (d)-(f) the z-component of the pulse for time instants $t_{1,2,3} = 7$, 9, 11 ns, considering the 17 to 21 GHz frequency range. The reference amplitude for the normalization is assumed at the first time instant $t_1 = 0.7$ ns. The pulse propagation is observed at $\phi = 0$, i.e, on xz-plane (note that all longitudinal planes are equivalent thanks to the azimuthal symmetry of the fields).

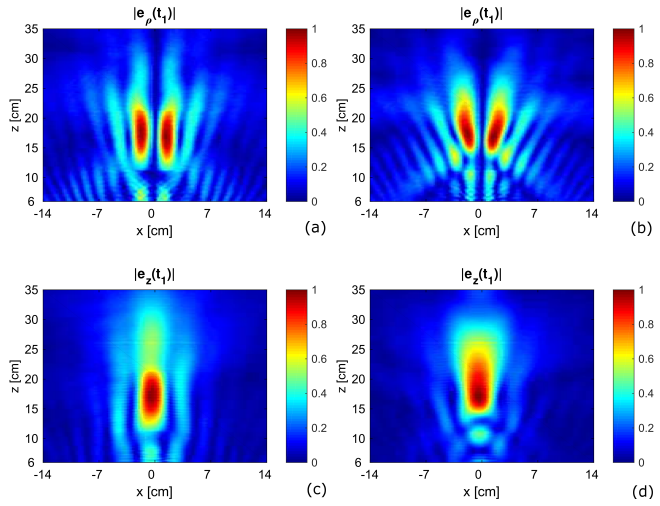

FIG. 4. Measured normalized leaky pulse field amplitude over the xz plane for (a)-(b) $|e_\rho|$, and (c)-(d) $|e_z|$. Comparison between leaky pulses obtained over two different fractional bandwidths for a fixed time instant $t_1 = 0.9$ ns. (a) and (c) FBW = 11.1% (i.e., 18 to 20 GHz); (b) and (d) FBW= 22.2% (i.e., 17 to 21 GHz).

file remains, indeed, well collimated for both the values of FBW, and along both the tranverse and longitudinal directions. However, the case achieved with the larger bandwidth (i.e., Figs. 4(b)-(d)) suffers from the presence of the wavenumber dispersion. The nondiffracting pulse, indeed, is slightly distorted and spoiled by the presence of tails. This effect is more visible as the pulse propagates further, approaching the nondiffracting range of the central frequency of 19 GHz (see also[11]).

To summarize, a planar radially-periodic LWA fed by a simple source has been proposed for generating limited-dispersive X-waves, by suitably selecting the operating bandwidth. As shown by the experiment, a fractional bandwidth of about 10% represents a good tradeoff among longitudinal localization and limited distortion, whereas a fractional bandwidth wider than 20% negatively affects the pulse shape during propagation. However, the presented prototype was not designed to have a limited cone dispersion, as suggested in[30], but to maximize the impedance bandwidth of the antenna, keeping the design as simple as possible. This and other aspects are worthy of further investigation. The use of larger fractional bandwidths, indeed, in conjunction with a controlled dispersion of the leaky-mode wavenumber, can potentially enable the generation of even shorter nondiffractive pulses at microwaves by means of simple planar devices. This is a very attractive and desirable feature that opens unprecedented possibilities for a wide class of practical applications. Both the longitudinal and transverse confinement of the pulse, indeed, could be of great interest for the design of next generation of high-resolution microwave and millimeter-wave holographic

imaging systems[48] and for the development of advanced electromagnetic non-destructive evaluation devices, with application to the field of ground penetrating radar and medical imaging[16,17,49,50]. As a matter of fact, most of the current techniques are based on pulsed radar systems (see, e.g.,[48]), which achieve the desired down-range resolution (i.e., longitudinal) transmitting a radio-frequency pulse. Cross-range resolution (i.e., transverse), instead, is typically achieved by relying on the size of the antenna footprint or, alternatively, by means of a synthetic aperture radar, SAR (see, e.g.,[48] and references therein). On this basis, thanks to both the transverse and longitudinal confinement of the pulse, X-waves could represent an attractive solution to obtain both down-range and cross-range high resolution in the near field without introducing a synthetic aperture, whilst taking advantages of the potential benefits (in term of power efficiency) given by the transmission of localized energy.

The authors would like to thank Mauro Ettorre, Guido Valerio, Matteo Albani, and Santi Concetto Pavone for the fruitful discussions on this topic.

[1] R. W. Ziolkowski, D. K. Lewis, and B. D. Cook, Phys. Rev. Lett. **62**, 147 (1989).
[2] A. M. Shaarawi, I. M. Besieris, and R. W. Ziolkowski, J. App. Phys. **65**, 805 (1989).
[3] R. W. Ziolkowski, Phys. Rev. A **39**, 2005 (1989).
[4] H. E. Moses and R. T. Prosser, SIAM J. App. Math. **50**, 1325 (1990).
[5] G. Scott and N. McArdle, Opt. Eng. **31**, 2640 (1992).
[6] W. Williams and J. Pendry, J Opt. Soc. Am. A **22**, 992 (2005).
[7] H. E. Hernández-Figueroa, M. Zamboni-Rached, and E. Recami, *Nondiffracting waves* (John Wiley & Sons, 2013).
[8] H. E. Hernández-Figueroa, M. Zamboni-Rached, and E. Recami, *Localized waves*, Vol. 194 (John Wiley & Sons, 2007).
[9] H. Sonajalg and P. Saari, Opt. Letters **21**, 1162 (1996).
[10] J. Durnin, J. Opt. Soc. Am. A **4**, 651 (1987).
[11] W. Fuscaldo, S. C. Pavone, G. Valerio, A. Galli, M. Albani, and M. Ettorre, J. Appl. Phys. **119**, 194903 (2016).
[12] J.-Y. Lu and J. F. Greenleaf, in *New Developments in Ultrasonic Transducers and Transducer Systems*, Vol. 1733 (International Society for Optics and Photonics, 1992) pp. 92–120.
[13] J. Y. Lu and J. F. Greenleaf, Ultrasonic Imaging **15**, 134 (1993).
[14] J. Yu Lu and S. He, Opt. Commun. **161**, 187 (1999).
[15] J. D. Heebl, M. Ettorre, and A. Grbic, Phys. Rew. App. **6**, 034018 (2016).
[16] R. J. Mahon, W. Lanigan, J. A. Murphy, N. Trappe, S. Withington, and W. Jellema, Proc. SPIE **5789**, 5789 (2005).
[17] H. Meng, B. Xiang, J. Zhang, W. Dou, and Y. Yu, J. Infrared Millim. Terahertz Waves **35**, 208 (2014).
[18] S. Mishra, Opt. Commun. **85**, 159 (1991).
[19] E. Recami, Physica A: Statistical Mechanics and its Applications **252**, 586 (1998).
[20] J. Salo, J. Fagerholm, A. T. Friberg, and M. Salomaa, Phys. Rev. E **62**, 4261 (2000).
[21] M. A. Porras, G. Valiulis, and P. Di Trapani, Phys. Rev. E **68**, 016613 (2003).
[22] J. Durnin, J. Opt. Soc. Am. A **4**, 651 (1987).
[23] D. McGloin and K. Dholakia, Contemp. Phys. **46**, 15 (2005).
[24] M. Ettorre, S. C. Pavone, M. Casaletti, M. Albani, A. Mazzinghi, and A. Freni, in *Aperture Antennas for Millimeter and Sub-Millimeter Wave Applications* (Springer, 2018) pp. 243–288.
[25] M. Lapointe, Opt. Laser Technol. **24**, 315 (1992).
[26] J.-Y. Lu and J. F. Greenleaf, IEEE Trans. Ultrason. Ferroelectr. Freq. Control **39**, 441 (1992).
[27] H. Sõnajalg, M. Rätsep, and P. Saari, Opt. letters **22**, 310 (1997).
[28] P. Saari and K. Reivelt, Phys. Rev. Lett. **79**, 4135 (1997).
[29] N. Chiotellis, V. Mendez, S. M. Rudolph, and A. Grbic, Phys. Rev. B **97**, 085136 (2018).
[30] W. Fuscaldo, D. Comite, A. Boesso, P. Burghignoli, P. Baccarelli, and A. Galli, Phys. Rew. App. (2018).
[31] C. Conti, S. Trillo, P. Di Trapani, G. Valiulis, A. Piskarskas, O. Jedrkiewicz, and J. Trull, Phys. Rev. Lett. **90**, 170406 (2003).
[32] C. Conti, Phys. Rev. E **68**, 016606 (2003).
[33] A. Couairon, E. Gaižauskas, D. Faccio, A. Dubietis, and P. Di Trapani, Phys. Rev. E **73**, 016608 (2006).
[34] M. A. Porras, G. Valiulis, and P. Di Trapani, Phys. Rev. E **68**, 016613 (2003).
[35] D. Comite, W. Fuscaldo, S. C. Pavone, G. Valerio, M. Ettorre, M. Albani, and A. Galli, App. Phys. Lett. **110**, 114102 (2017).
[36] D. Comite, G. Valerio, M. Albani, A. Galli, M. Casaletti, and M. Ettorre, IEEE Trans. Antennas Propag. **65**, 2123 (2017).
[37] M. Q. Qi, W. X. Tang, and T. J. Cui, Sci. Rep. **5**, 11732 (2015).
[38] B. G. Cai, Y. B. Li, W. X. Jiang, Q. Cheng, and T. J. Cui, Opt. Express **23**, 7593 (2015).
[39] Y. C. Zhong and Y. J. Cheng, IEEE Trans. Antennas Propag. **65**, 5035 (2017).
[40] D. Comite, W. Fuscaldo, S. K. Podilchak, V. Gómez-Guillamón Buendía, P. D. Hilario Re, P. Burghignoli, P. Baccarelli, and A. Galli, IEEE Trans. Antennas Propag. **66**, 1 (2018).
[41] Z. Li, K. B. Alici, H. Caglayan, and E. Ozbay, Phys. Rev. Lett. **102**, 143901 (2009).
[42] M. Albani, S. C. Pavone, M. Casaletti, and M. Ettorre, Opt. Express **22**, 18354 (2014).
[43] S. C. Pavone, M. Ettorre, M. Casaletti, and M. Albani, Opt. Express **24**, 11103 (2016).
[44] S. C. Pavone, A. Mazzinghi, A. Freni, and M. Albani, Opt. Express **25**, 19548 (2017).
[45] S. K. Podilchak, P. Baccarelli, P. Burghignoli, A. P. Freundorfer, and Y. M. Antar, IEEE Trans. Antennas Propag. **62**, 2978 (2014).
[46] M. Abramowitz and I. A. Stegun, *Handbook of Mathematical Functions* (New York: Dover, 1962).
[47] P. Baccarelli, S. Paulotto, D. R. Jackson, and A. A. Oliner, IEEE Trans. Microw. Theory Tech. **55**, 1484 (2007).
[48] J. Hunt, J. Gollub, T. Driscoll, G. Lipworth, A. Mrozack, M. S. Reynolds, D. J. Brady, and D. R. Smith, J. Opt. Soc. Am. A **31**, 2109 (2014).
[49] A Mazzinghi, M. Balma, D. Devona, G. Guarnieri, G. Mauriello, M. Albani, and A. Freni, IEEE Trans. Antennas Propag. **62**, 3911 (2014).
[50] J. Y. Lu and J. F. Greenleaf, IEEE Trans. Ultrason. Ferroelectr. Freq. Control **37**, 438 (1990).